On temperature-dependent experimental *I-V* and *C-V* data of Ni/*n*-GaN Schottky contacts

Nezir Yıldırım,[1] Kadir Ejderha,[1] and Abdulmecit Turut[2,a)]
[1]*Department of Physics, Faculty of Sciences and Arts, Bingöl University, 12000 Bingöl, Turkey*
[2]*Department of Physics, Faculty of Sciences and Arts, Ataturk University, 25240 Erzurum, Turkey*

(Received 5 May 2010; accepted 25 October 2010; published online 8 December 2010)

We report the current-voltage (*I-V*) and capacitance-voltage characteristics (*C-V*) of Ni/*n*-GaN Schottky diodes. Gallium nitride is a highly promising wide band gap semiconductor for applications in high power electronic and optoelectronic devices which require Schottky barriers for modulating the channel mobile charge. The *I-V* and *C-V* characteristics of the diodes have been measured in the temperature range of 80–400 K with steps of 20 K. Thermal carrier concentration and barrier height versus temperature plots have been obtained from the C^{-2}-*V* characteristics, and a value of $\alpha=-1.40$ meV/K for temperature coefficient of the barrier height. The modified activation energy plot according to the barrier inhomogeneity model has given the Richardson constant A^* as 80 or 85 A/(cm^2 K^2). © *2010 American Institute of Physics*.
[doi:10.1063/1.3517810]

I. INTRODUCTION

GaN is an attractive compound semiconductor used in optoelectronic and microelectronic device applications, such as GaN-based light-emitting diodes (LEDs) and laser diodes (LDs), ultraviolet (UV) detectors and high temperature, high power and high frequency electronic devices.[1–12] GaN has a wide direct band gap of 3.4 eV at room temperature. This makes a wide range of band gap available for electronic and optoelectronic devices.[1–7] Metal-semiconductor (MS) rectifier contacts are fundamental units of both high power GaN rectifiers and high electron mobility transistors. However, the rectifying contacts on GaN with a high and ideal Schottky barrier height (SBH) and a low leakage current and their physical origin still have a serious technological concern and continuously object of investigation.[6,10–19]

Sawada *et al.*[14] have studied the capacitance-voltage (*C-V*) measurements at room temperature and current-voltage-temperature (*I-V-T*) in Ni/*n*-GaN Schottky diodes formed on oxide-etched or thermally oxidized surfaces, and their results have supported existence of surface patches with low SBH which cause a leakage current of the Schottky structures. Yu *et al.*[16] have investigated the carrier transport mechanism for Ni/*n*-GaN Schottky barrier diodes (SBDs) using the *I-V* characteristics as function of temperature and *C-V* characteristics at room temperature, and they[16] have concluded that the enhanced tunneling effect due to defects near the surface region is a likely cause for the large scattering in the Richardson constant measured by the *I-V-T* method. Guo *et al.*[17] have measured the SBH by *I-V* and *C-V* methods at room temperature of Ni/*n*-GaN SBDs annealed at various temperatures from 100 to 400 °C for 20 min in a nitrogen ambient mixed with hydrogen to study their thermal stability, and concluded that formation of the nickel nitrides should affect the measured SBH. Iucolano *et al.*[18] have investigated the temperature dependence of the forward bias *I-V* characteristics, in temperature range of 25–175 °C, of Ni/*n*-GaN Schottky contacts annealed at 500 °C. The systematic studies on the electrical behavior of metal/GaN Schottky contacts are always important to acquire a deeper knowledge of the Schottky diode parameters and of the current transport mechanisms. Generally, analysis of the *I-V* and *C-V* characteristics of the SBDs at room temperature does not give detailed information about their conduction process or the nature of barrier formation at the MS interface. The temperature dependence of the *I-V* and *C-V* characteristics allows us to understand different aspects of conduction mechanisms.[1,6,20–25] In this work, a detailed analysis of the *I-V* and *C-V* characteristics of Ni/*n*-GaN Schottky contacts has been carried out to clarify the origin of the anomalous behavior of temperature dependence of the Schottky diode parameters such as the SBH and ideality factor and the Richardson's constant. Our results have been explained on the basis of a thermionic emission (TE) mechanism with lateral inhomogeneities at the Ni/*n*-GaN interface.

The SBH is expected to be dependent on the metal work function due to the ionic nature of *n*-type GaN. Metals with a high work function such as Pt, Ni, Pd, and Au are used for Schottky contacts to *n*-type GaN, according to Mott–Schottky relation.[3–6,16,17,20,21] Furthermore, the chose of Ni allows the formation of high resistance, large work function, and thermally stable metallic compounds.[3] Moreover, pure Ni exists on the surface of the Ni/*n*-GaN contacts even after RTA at high temperatures, in contrast, the same Ni in Au/Ni/*n*-GaN is completely transformed into NiO by RTA at 500 °C.[3] This is important for our own Ni/*n*-GaN sample whose *I-V* and *C-V* measurements have been made in the temperature range of 80–400 K. Considering the metal work function Φ_m, the theoretical Schottky–Mott BH in metal/*n*-type semiconductor contacts is given by $q\Phi_{bn}=(q\Phi_m-\chi_s)$, where $\Phi_m=5.15$ V for Ni and χ_s is the electron affinity of the semiconductor and equals 4.11 eV for GaN.[3,5] As can be seen, the BH increases with increasing Φ_m for a

a)Electronic mail: aturut@atauni.edu.tr.

given n-type semiconductor. According to the equation above, $q\Phi_{bn}=1.04$ eV in the Ni/n-GaN contacts. In most practical MS contacts, the ideal situation is never reached because the BH is often influenced by the interfacial interactions.[3–6,16–25] The observation suggests that the work function of metal is not the exclusive factor determining the SBH on GaN.[3–6,16,17] For example, Sawada *et al.*[14] and Guo *et al.*[16] and Yu *et al.* have obtained the BH values of 0.81 eV, 0.66 eV and 0.88 eV for Ni/n-GaN SBD at 300 K, respectively, and Arulkumaran *et al.*[25] a value of 0.91 eV. Therefore, it can be said that the BH in Schottky contacts is likely a function of the interface atomic structure, and the atomic inhomogeneities at the MS interface which are caused by grain boundaries, multiple phases, facets, defects, a mixture of different phases etc.[1–6,22–38] The contaminants at the MS interface may also act directly to introduce inhomogeneity through the generation of defects. The potential fluctuations may also originate from a local effective barrier lowering due to field emission at metallic diffusion spikes with narrow radii of curvature.[1–6,21–38]

II. EXPERIMENTAL DETAILS

GaN used for this study was supplied from University Wafer. GaN epitaxial layer with a free carrier density of 9×10^{16} cm^{-3} (as received from the manufacturer) was grown on a (0001) Al_2O_3 c-plane substrate by metalorganic chemical vapor deposition (MOCVD) and the thickness of the GaN epitaxial layer was 2 μm. Before Ohmic contact fabrication, the samples were cleaned by first boiling them in aqua regia (HNO_3:HCl=1:3) and rinsing in deionized water, then a degreasing process followed by boiling in trichloroethylene, then rinsing in boiled izopropanol, and thereafter, in deionized water. Finally, the samples were dipped in HCl:H_2O (1:1) for 10 s. After this cleaning, Ti Ohmic contact was fabricated on the GaN and annealed at 700 °C for 3 min flowing N_2 in a quartz tube furnace.[8] Prior to Schottky contact fabrication, the samples were again degreased and dipped in an HCl:H_2O (1:1) solution to remove oxides and hydroxides formed on the GaN surface. Then, the circular Ni Schottky contacts 1.5 mm in diameter and 100 nm in thickness were successfully fabricated. The Schottky metallization of Ni was deposited by magnetron DC sputtering. Since the sapphire substrate is insulating, both Ohmic and Schottky contacts were made on the same surface of the GaN. Gallium oxides and hydroxides form on the GaN surface and grow rapidly on the nitride surface when it is exposed to air, and unless these are removed prior to metal deposition, these oxides and hydroxides would create an interfacial layer between the MS interface. Such surface oxides are serious impediment to making ideal metal contacts to nitrides. Aqua regia removes much of the surface oxide layer.[3–6,16–21] Temperature-dependent I-V and C-V measurements on Ni/n-GaN SBDs were carried out in the range 80–400 K.

III. RESULTS AND DISCUSSION

A. Capacitance-voltage characteristics

The reverse and forward C-V characteristics were studied with a computer-controlled HP 4192A LF Impedance Analyzer. Figures 1 and 2 show the experimental forward and reverse bias C-V and C^{-2}-V curves, respectively, of the Ni/n-GaN SBD in the temperature range of 80–400 K at 500 kHz. In Schottky diodes, the depletion layer capacitance can be expressed as[20,21]

$$C^{-2}=2\left(V_{do}+V-\frac{kT}{q}\right)/(q\varepsilon_s A^2 N_d), \tag{1}$$

where A is the Schottky contact area, V_{d0} is the diffusion potential, N_d is the carrier concentration obtained from the slope of the linear portion of the C^{-2}-V plot and $+V$ is the reverse bias voltage. Under the applied reverse bias, the electrode of the Ohmic contact was positively biased with respect to the Ni electrode (Schottky contact).

From Eq. (1), the slope of the forward and reverse bias C^{-2}-V curves is given by

$$\frac{d(C^{-2})}{dV}=\frac{2}{q\varepsilon_s A^2 N_d}. \tag{2}$$

The diffusion potential V_{d0} is determined from the extrapolation of the linear C^{-2}-V plot to the V axis, and the negative intercept $-V_0$ on the V axis equals to $-V_{d0}+(kT)/q$, as can be seen in Fig. 2, so that $V_{d0}=V_0+kT/q$. The linear fits to calculate N_d and flat-band BH $\Phi_{C\text{-}V}$ were made to the experimental data in approximately (–0.20)-(+1.0) V range. The BH from the C^{-2}-V curves is given by $\Phi_b^{cv}=V_{d0}+V_n$, V_n is

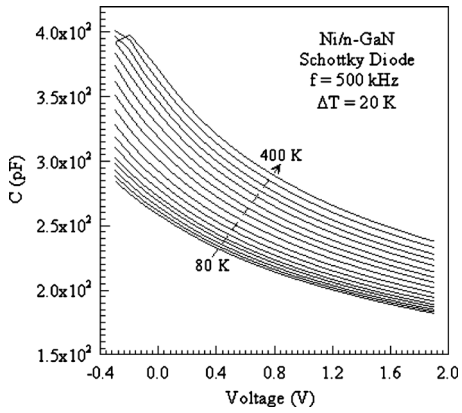

FIG. 1. Forward and reverse bias C-V characteristics for Ni/n-GaN Schottky diode in the temperature range of 80–400 K.

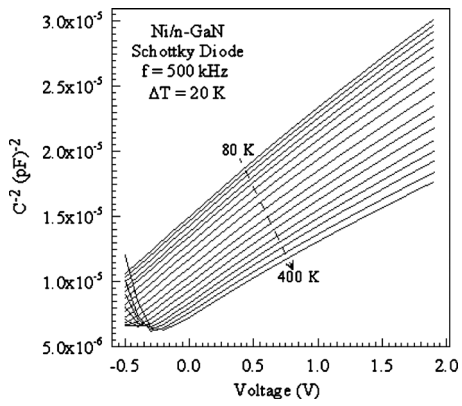

FIG. 2. Forward and reverse bias C^{-2}-V characteristics for Ni/n-GaN Schottky diode in the temperature range of 80–400 K from Fig. 1.

the potential difference between the Fermi level and minimum of the conduction band for n-GaN in the neutral region, and it can be calculated from the following relation:

$$V_n = \frac{kT}{q}\ln\left(\frac{N_c}{N_d}\right), \tag{3}$$

where N_c is the state density in the conduction band for n-GaN, $N_c = 2.38 \times 10^{18}$ cm^{-3} at room temperature and has a temperature dependence of $N_c \alpha T^{3/2}$. The temperature-dependent experimental values of N_d and N_c were used in the calculations.

The experimental C^{-2}-V plot at each temperature is not fully linear. It may be explained the causes of slight nonlinearity along curve. The slight nonlinearity of the C^{-2}-V curves indicates that the carrier concentration is almost nonuniform. From only the linearity of the C^{-2}-V curves in (−0.20)-(+1.0) V range, it is not apparent if the Schottky diode suffers from the presence of traps and/or surface states. Figure 2 shows according to Eq. (2) how the value of N_d increases as the slope of the C^{-2}-V curves decreases. The local slope of the C^{-2}-V curves decreases gradually with increasing bias, indicating an increase in N_d with increasing bias and depth. This case indicates the presence of donorlike deep traps (i.e., neutral when occupied, positively charged when empty) within the space-charge region. The charge state of the donorlike traps will depend on the position of the Fermi level. Let us consider a Schottky barrier in an n-type semiconductor. The traps will be occupied by electrons if they lie below the Fermi level and will be empty above the Fermi level. In metal/n-type semiconductor contacts, the space charge Q_{sc} charge is the positive due to the uncompensated donors. When the diode is under the reverse biased, the space charge region increase more than its equilibrium value and the donorlike deep trap levels emerge above the Fermi level. Consequently, some trapped electrons are no more in equilibrium and emitted into the conduction band. Thus, the positive charge quantity in the depletion region increases due to ionized defect centers. So, it can be stated that the slope of C^{-2}-V plot or the carrier concentration changes appreciably. Moreover, the experimental plots of Fig. 2 indicate that, the capacitance for a certain voltage V increases with increasing temperature. This is clearly reflected from Eq. (1). As can be well-known, there will be an additional contribution to capacitance and thus to the doping concentration because the deep-level traps emit more electrons at higher temperatures.

Figure 3 shows the BH versus temperature plot from the C^{-2}-V characteristics for Ni/n-GaN Schottky diode in the temperature range of 80–400 K. The value of $\Phi_{C\text{-}V}$ was obtained from the linear fits to the experimental data in approximately (−0.20)-(+1.0) V range of the C^{-2}-V plots. The value of $\Phi_{C\text{-}V}$ ranges from 1.54 V at 300 K to 1.90 eV at 80 K. The experimental $\Phi_{C\text{-}V}$ versus T plot yields the values of $\Phi_{C\text{-}V}$ (T=0)=2.04 V for the BH and $\alpha = -1.40$ meV/K for the BH temperature coefficient. The BH $\Phi_{C\text{-}V}$ from the C^{-2}-V decreases as the temperature increases. Generally, the temperature dependence of the Schottky BH should follow the temperature dependence of the band gap with a coefficient almost identical to that of the band gap.[39–43] The band gap shrinks at higher temperature. If it is assumed that the

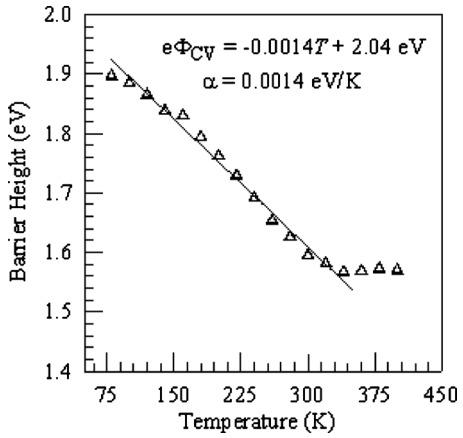

FIG. 3. BH vs temperature plot from the C^{-2}-V characteristics for Ni/n-GaN Schottky diode in the temperature range of 80–400 K, the solid line represents the fit to the experimental data.

conduction band edge shifts downward, the valence band edge shifts upward during this shrinkage, and that these two shifts are equal and opposite.[21,39] The BH temperature coefficient of $\alpha = -1.40$ meV/K is in close agreement with temperature coefficient of −1.08 meV/K of the band gap.[39] That is, such a temperature dependence implies the Fermi level is pinned to the bottom of the valance band at the MS interface due to defects.[39–43]

Moreover, the temperature dependence of the experimental carrier concentration (N_d) was calculated from the reverse bias C^{-2}-V characteristics in Fig. 2, and the N_d versus $1/T$ plot is given in Fig. 4. For example, these values were 5.90×10^{15} and 8.50×10^{15} cm^{-3} for the n-type GaN wafer at 80 and 400 K. The carrier concentration of 9×10^{16} cm^{-3} received from the manufacturer is higher than value of 7.10×10^{15} cm^{-3} obtained from the C-V measurement at room temperature (about 300 K). As can be seen from Fig. 4, the carrier concentration of the n-GaN slightly decreases with a decrease in temperature in the range of 80–280 K while it more decreases with a decrease in temperature in the range of 280–400 K. At very low temperatures, most impurities are frozen out. Especially, Fig. 4 depicts that the carrier concentration increases with temperature and that it becomes very sensitive to temperature at temperatures about

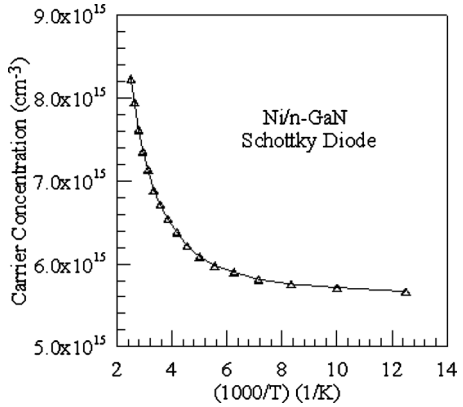

FIG. 4. Thermal carrier concentration vs temperature plot from the C^{-2}-V Characteristics for Ni/n-GaN Schottky diode in the temperature range of 80–400 K, the solid line represents the fit to the experimental data.

250 K. The reason is that almost all the donors are ionized and the deep-level traps emit more electrons with an increase in temperature, and thus the carrier concentration increases.

As can be seen from Fig. 2, the decrease in the slope of the C^{-2}-V curve with increasing reverse bias at a given temperature is a clear evidence for the explanation above. As will be understood from explanations above, the clean semiconductor suffer from the influence of deep trap states and the reaction products formed by as-deposited metal film on semiconductor. Therefore, it is not possible to deduce by only depletion approximation whether the material is compensated or not, so the profile N_d can only be regarded as the net carrier concentration. The origin of the difference may be from vacancies induced by the interfacial reactions between Ni and n-GaN.[3,6,13,17] As mentioned in Refs. 3 and 17, Ga_4Ni_3 can form due to the as-deposited Ni film on GaN. The formation of Ga_4Ni_3 and Ga_3Ni_2 accompanies the accumulation of Ga vacancies in the GaN subsurface. Accumulation of Ga vacancies leads to a decrease in the n-doping level.[3]

B. Current-voltage (I-V) characteristics

To understood whether or not a Schottky diode has the ideal diode behavior we analyze its experimental I-V characteristics by the forward bias TE theory given as follows[20]

$$I = I_0 \exp\left[\frac{q(V-IR)}{nkT}\right]\left\{1-\exp\left[-\frac{q(V-IR)}{kT}\right]\right\}, \quad (4)$$

where I_0 is the saturation current derived from the straight line intercept of $\ln I$ at $V=0$ and it is given by

$$I_0 = AA^*T^2 \exp\left(-\frac{q\Phi_{ap}}{kT}\right), \quad (5)$$

q is the electron charge, V is the forward-bias voltage, A is the effective diode area, k is the Boltzmann constant, T is the absolute temperature, A^* is the effective Richardson constant of 26.8 A cm^{-2} K^{-2} for n-type GaN,[6] R_s is the series resistance of the neutral region of the semiconductor bulk (between the depletion region and Ohmic contact), IR_s is the voltage drop across the series resistance, $q\Phi_{ap}$ is the experimental zero-bias apparent BH and n is the ideality factor. From Eq. (4), ideality factor n can be written as

$$n = \frac{q}{kT}\left(\frac{dV}{d\ln I}\right). \quad (6)$$

The temperature dependence of the I-V characteristics was measured in the temperature range of 100–400 K using a closed-cycle helium cryostat, and a Keithley 487 Picoammeter/Voltage Source in the dark. Figure 5 shows the experimental semilog forward and reverse bias I-V characteristics of the Ni/n-GaN Schottky contact in the temperature range of 100–400 K with steps of 20 K. The BH and n have been evaluated from the upper part with higher BH of the temperature-dependent forward bias I-V characteristics from 100 K to 400 K. An experimental BH value of 0.82 eV (300 K) for the Ni/n-GaN SBD was calculated by the help of Eq. (5) from the current-axis intercepts of the semilog-forward bias I-V plots in Fig. 5, and an experimental value of 1.98 (300 K) for n using Eq. (6).

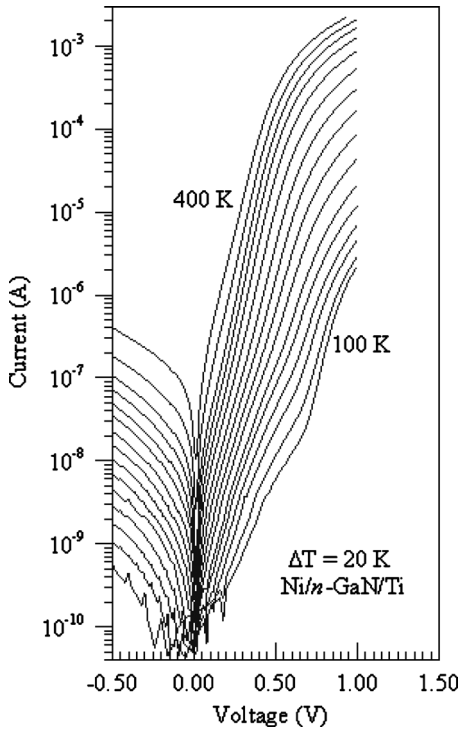

FIG. 5. Semilog forward and reverse bias I-V characteristics for Ni/n-GaN Schottky diode in the temperature range of 100–400 K.

The value of 0.82 eV is lower than the value of 1.04 eV calculated according to the theoretical Schottky–Mott model. This is due to the fact that the Schottky behavior is significantly affected by the interfacial interactions between the Ni and GaN.[3,16,17,20,21] Ga_4Ni_3 forms as Ni is deposited on GaN, and it is responsible for the low BH of the as-deposited Ni film on GaN.[3,17] The value of 0.82 eV for the Ni/n-GaN at 300 K is in close agreement with value of 0.81 eV given for the Ni/n-GaN SBD at 300 K by Sawada *et al.*[14] As expected, the C^{-2}-V curve gave BH values higher than those derived from I-V measurements. This is due to the different nature of the I-V and C-V measurement techniques. The C-V method gives the flat-band BH, whereas the I-V method yields the zero-bias BH. In general, the flat-band BH is a better measure of the BH than the zero-bias BH. The capacitance is insensitive to potential fluctuations on a length scale of less than the space charge region and the C-V method averages over the whole Schottky area and results in a homogeneous BH. The dc across the interface exponentially depends on the BH.[7,18–23] That is, the current in the I-V measurement is dominated by the current which flows through the region of low BH. Therefore, the measured I-V BH is significantly lower than the weighted arithmetic average of the BHs. The BH determined from the C^{-2}-V curve is close to the weighted arithmetic average of the BHs.[7,22,23]

The BH and ideality factor versus temperature plot is given in Fig. 6. A dependence of the ideality factor n and BH on the temperature is clearly being seen in Fig. 6. That is, Fig. 6 indicates that the BH increases and the ideality factor decreases with an increase in temperature. It should be men-

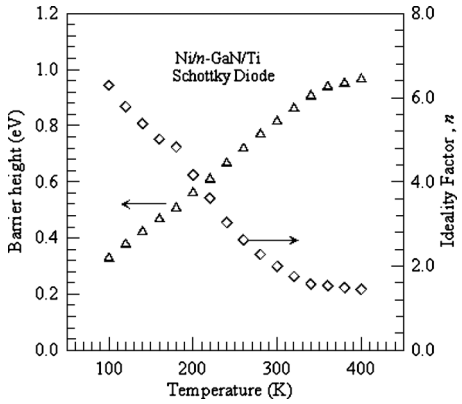

FIG. 6. BH and ideality factor vs temperature plot from the forward bias *I-V* characteristics for the Ni/*n*-GaN Schottky diode in the temperature range of 100–400 K.

tioned an important point here. As temperature increases, there occurs inter-diffusion and atomic/electronic reorganization inside the contact. The increase in temperature up to 400 K thus serves the purpose of annealing. So, the atomic structure of the contact becomes more robust, Fowler–Nordheim tunneling becomes lower, and the (Ni, Ga, and N) alloy exhibits higher metal work function with respect to the electron affinity of the semiconductor. The immediate result of all these is the increase in BH and decrease in ideality factor.[39]

Such a temperature behavior both of the BH and *n* is commonly observed in "reel" Schottky diodes. The nonideal behavior is probably due to surface defect or to local enhancement of electric field which can also yield a local reduction of the BH which leads to inhomogeneities in the transport current.[22–35] The other reasons of the barrier inhomogeneity can arise from the different interface quality, which, in turn, depends on several factors such as the surface defects density, the surface treatment (cleaning, etching, etc.), the metal and the deposition process (evaporation, sputtering, etc.), etc.[6–9,14,22–27] Arehart *et al.*[27] have reported that Ni/*n*-GaN Schottky diodes with the lower threading dislocation density (TDD) shows nearly ideal Schottky behavior. However, the Schottky diode with higher TDD displays significant deviations in the detailed *I-V* characteristics that are explained by the influence of an inhomogeneous Ni/*n*-GaN interface.

Likewise, as can be seen from Fig. 5, the current in the small bias region at low temperatures exceeds significantly that predicted by the TE model, and the low temperature *I-V* characteristics cannot be fitted by Eq. (1) at the whole bias region. As well-known, the electrons in the metal by only TE must have sufficient energy to surmount the BH. This does not occur until the applied gate bias is high enough to energize a sufficient number of electrons with energy BH. This is why we did not observe thermionic emission at low applied bias and temperatures. However, due to the wide band gap of the GaN, the other current component such as TFE and carrier recombination might dominate the carrier transport at low temperature. At low temperatures, the current through the diode is the sum of the thermionic current flowing through patches of low BH together with the trap-assisted tunneling.[1,6–9,15,22–28] As explained in Ref. 1, the trap-assisted tunneling can take place by the traps localized in various energy states within the energy band gap. There will effectively be the trap-assisted tunneling through the Schottky barrier if the localized states within the energy band gap are sufficiently energetic or the Schottky barrier width is smaller than a certain critical width. The reduction in the barrier width may take place if there are the nitrogen vacancies in sufficient number at the MS interface due to the influence of the applied gate bias. The nitrogen vacancies can then act as dopant atoms lowering the conduction band edge. Thus, the trap-assisted tunneling can take place if the applied gate bias is sufficient enough to cause band bending of the conduction band. At high temperatures, such as in the temperature range of 240–400 K in Fig. 5, the current flow is less dominated by the small number of low-BH regions, and the current flow through the uniform region accounts for most of the total current.[1,6–9,15,22–28] In addition, in the case where the current density at low barrier patch is higher than the current density at the uniform regions, the series resistance becomes important in the low barrier patches at lower values of bias at the low temperature *I-V* characteristics.

Moreover, the temperature dependence of the measured BH from the forward bias *I-V* is usually explained in terms of the temperature dependence of the semiconductor band gap, as in the BH determined from the C^{-2}-*V* curve. However, it is sometimes found that the temperature coefficient of the BH differs substantially from the band-gap temperature coefficient and is often of the opposite sign. The BH from the *I-V* curves decreases with a decrease in temperature, this is attributed to inhomogeneous MS contacts. In our case, the current transport will be dominated by current flowing through the patches of the lower BH with larger ideality factor at low temperatures as a result of the inhomogeneous MS contacts. As a result, the dominant BH from the forward bias *I-V* characteristics will increase with the temperature and bias voltage due to barrier inhomogeneity in MS interface.[22–24,40–44] This may be the reason of why the characteristics of the BH versus temperature plot from the *C-V* measurements are completely opposite to those from the *I-V* measurements.

Moreover, the "soft" or slight nonsaturating behavior observed as a function of bias in the experimental reverse bias branch in Fig. 5 may be explained in terms of the spatial inhomogeneity of BH.[22–25] The bias dependence of the SBH is frequently observed experimentally. However; in many cases, the bias dependence of the BH determined from the reverse bias characteristics exceeds the expected result related to image force lowering. The existence of BH inhomogeneity offers a natural explanation for the soft reverse characteristics observed experimentally.[22–25] For inhomogeneous MS contacts, the reverse current may be dominated by the current which flows through the low-BH patches.

The linearity of the BH versus $1/T$ curve (the open triangles) in Fig. 7 shows the temperature-dependent data of the Ni/*n*-GaN Schottky contact. This plot obeys to model which is the related to TE over a Gaussian BH distribution given with the following expression:[23,24,28–32]

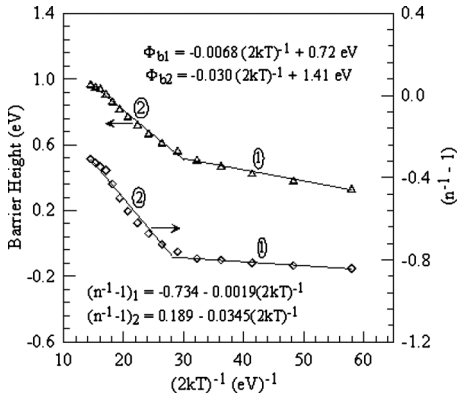

FIG. 7. Zero-bias apparent BH (the open triangles) and ideality factor (the open squares) vs $1/(2kT)$ curves of the Ni/*n*-GaN Schottky contact according to double-Gaussian distributions of BHs. The data show linear variation in the two temperature ranges with a transition around 200 K.

$$\Phi_{ap} = \bar{\Phi}_{bo} - \frac{q\sigma_{so}^2}{2kT}, \tag{7}$$

where Φ_{ap} is the experimentally measured apparent BH from the forward bias *I-V* characteristics and σ_{so} is the zero bias standard deviation of the BH distribution and it is a measure of the barrier homogeneity. The temperature dependence of σ_{so} is usually small and can be neglected. The BH has a Gaussian distribution with the zero bias mean BH $\bar{\Phi}_{bo}$. The deviation from classical TE theory can be explained by a spatial fluctuation of the BH at interface.[6,7,22–33] As stated by Iucolano *et al.*;[6] Werner and Güttler[23] and Song *et al.*[24] assume a continuous spatial distribution of the barrier; and the total current across a Schottky diode is obtained by integrating the TE current expression with an individual BH and weighted by using the Gaussian distribution function. This approach, however, does not consider the lateral length scale of the inhomogeneity and the pinch-off effect related to the interaction between adjacent regions with different. The approach points out that the apparent BH is always lower than the mean value of the barrier distribution.

The variation in ideality factor n_{ap} with temperature in the model is given by[23,28]

$$\left(\frac{1}{n_{ap}} - 1\right) = -\rho_2 + \frac{q\rho_3}{2kT}, \tag{8}$$

where

$$\Delta\bar{\Phi}_b(V,T) = \bar{\Phi}_b(V,T) - \bar{\Phi}_b(0,T) = \rho_2 V, \tag{9}$$

$$\Delta\sigma^2(V) = \sigma^2(V) - \sigma^2(0) = \rho_3 V. \tag{10}$$

The voltage-independent ideality factor *n* requires a linear increase in $\Phi_b(V,T)$ with the bias. This is only possible if the mean BH $\bar{\Phi}_b$ as well as the square of the standard deviation σ^2 vary linearly with the bias.[23,28,36–38] As can be seen from Eqs. (8)–(10), ρ_2 is the voltage coefficient of the mean BH, and ρ_3 is the voltage coefficient of the standard deviation. According to Eq. (8), a plot of $(n^{-1}\text{-}1)$ against $1/T$ should give a straight line with the slope and *y*-axis intercept related to the voltage coefficients ρ_2 and ρ_3, respectively. The value of ρ_3 indicates that the distribution of the BH becomes more homogeneous with voltage increase.

The experimental $[(1/n_{ap})\text{-}1]$ versus $1/T$ (the open squares) and Φ_{ap} versus $1/T$ (the open triangles) plots in Fig. 7 correspond to two lines instead of a single straight line with transition occurring at 200 K. The values of ρ_2 obtained from the intercepts of the experimental $[(1/n_{ap})\text{-}1]$ versus 1/T plot are −0.189 in 200–400 K range, and 0.734 in 100–200 K range, and the values of ρ_3 from the slopes are −0.0345 V in 200–400 K range, and −0.0019 V in 100–200 K range. The intercept and slope of the straight line have given two sets of values of $\bar{\Phi}_{bo}$ and σ_{so} as 1.41 V and 173 mV in the temperature range of 200–400 K, respectively, and as 0.72 V and 82 mV in the temperature range of 100–200 K, respectively. As can be seen from the explanations above, the temperature dependence of the experimental values of BH of the Ni/*n*-GaN has been described by two Gaussian distributions in the temperature range of 80–400 K. Two Gaussian distributions and standard deviation values obtained for the Ni/*n*-GaN SBD are similar to the results obtained for Pd/*n*-GaN and Pt/*n*-GaN in the temperature range of 80–400 K.[7] Therefore, the above result again suggests that the origin of barrier inhomogeneity in M/GaN SD is a property of the semiconductor substrate rather than the deposited metal. The physical implication of the fact that the intercept and slope of the straight line have given two sets of values of the BH and σ_{so} may be supplied from the domination of two different mechanisms (trap-assisted tunneling and thermionic emission) for carrier transport in two different temperature ranges.[1,7]

The conventional activation energy $\ln(I_0/T^2)$ versus $1/T$ plot [Eq. (5)] based on the TE current mechanism have showed nonlinearity at low temperatures (not given here). Therefore, a modified activation energy plot according to the Gaussian distribution of the BHs has been given. Zhou *et al.*[26] found that the value of A^* determined by a modified Richardson's plot in the GaN material is close to the theoretical value. On the other hand, clearly, the wide range of variability of these results can be ascribed to the surface defect density, the surface treatment and the metal deposition process.[6] As an example, Arehart *et al.*[27] observed a dependence of A^* on the dislocation density of the material in Ni/*n*-GaN Schottky diodes, and obtained a value of 23 $A/(cm^2\,K^2)$ for the devices with the lower TDD. When considering Eqs. (5) and (7), an expression for the modified activation energy plot according to the Gaussian distribution of the BHs can be rewritten as

$$\ln\left(\frac{I_0}{T^2}\right) - \left(\frac{q^2\sigma_s^2}{2k^2T^2}\right) = \ln(AA^*) - \frac{q\bar{\Phi}_{bo}}{kT}. \tag{11}$$

Using the experimental I_0 data, the modified $\ln(I_0/T^2)\text{-}q^2\sigma_{so}^2/2k^2T^2$ versus $1/T$ plot can be obtained according to Eq. (11). This plot should give a straight line with slope directly yielding the mean $\bar{\Phi}_{bo}$ and the intercept $(=\ln AA^*)$ at the ordinate determining A^* for a given diode area *A*. The $[\ln(I_0/T^2)\text{-}q^2\sigma_{so}^2/2k^2T^2]$ values were calculated using both two values of σ obtained for the temperature

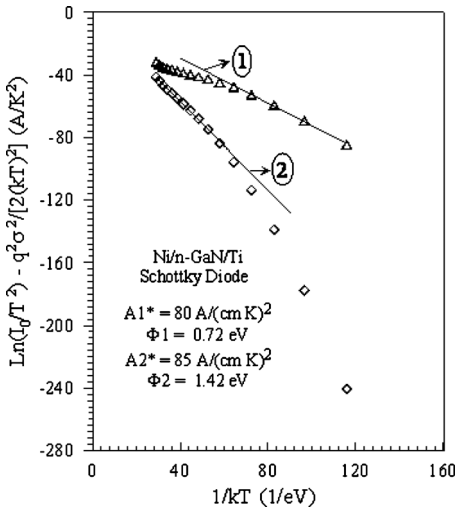

FIG. 8. Modified Richardson plot, $\ln(I_0/T^2)$-$q^2\sigma_{so}^2/2k^2T^2$ vs $1/T$, for the Ni/n-GaN Schottky diode according to the double-Gaussian distributions of BHs. The open triangles represent the plot calculated for σ_{so}=82 mV (the straight line 1) in temperature range of 100–200 K, and the open squares represent the plot calculated for σ_{so}=173 mV (the straight line 2) in temperature range of 200–400 K

ranges of 100–200 and 200–400 K. Thus, in Fig. 8, the open triangles represent the plot calculated with σ_{so}=82 mV (the straight line 1) in temperature ranges of 100–200 K, and the open squares represent the plot calculated with σ_{so}=173 mV (the straight line 2) in temperature ranges of 200–400 K. The best linear fits to the modified experimental data are depicted by solid lines in Fig. 8 which represent the true activation energy plots in respective temperature ranges. The calculations have yielded zero bias mean BH $\bar{\Phi}_{bo}$ of 0.72 eV (in the range of 100–200 K) and 1.42 eV (in the range of 200–400 K). These values match exactly with the mean BHs obtained from the Φ_{ap} versus $1/T$ plot in Fig. 7. The value of 1.42 eV in the range of 200–400 K is in close agreement with the experimental value of $\Phi_{C\text{-}V}$=1.54 eV from the C^{-2}-V characteristics at 300 K in Fig. 3. In Fig. 8, the intercepts at the ordinate give the Richardson constant A^* as 80 A/(cm^2 K^2) (in 100–200 K range) and 85 A/(cm^2 K^2) (in 200–400 K range) without using the temperature coefficient of the BHs.

According to Eq. (7), Φ_{ap} increases with increasing temperature. Equation (5) is a complex function of temperature. I_0 tends to increase with increasing temperature. But the same I_0 tends to decrease with increasing Φ_{ap} which is due to increase in temperature. This suggests that a theoretical plot of the current with temperature is needed in order to resolve the ambiguity of the experimental temperature-dependence of the current, and to demonstrate that this temperature dependence follows Eq. (7). To resolve this ambiguity, the expression of the bias- and temperature-dependent BH $\Phi_b(V,T)$ and bias-dependent standard deviation given for the Gaussian distribution has been used:[36,38]

$$\Phi_b(V,T) = \bar{\Phi}_b(0,T) - \frac{q\sigma^2(0)}{2kT} + \left(\rho_2 - \frac{q\rho_3}{2kT}\right)V, \qquad (12)$$

where V is the forward bias voltage. At first, it has been obtained the theoretical BH versus temperature plots from

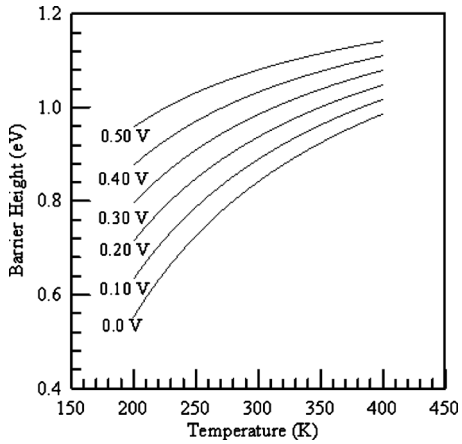

FIG. 9. Theoretical BH vs temperature plots from 200 to 400 K as a function of forward bias according to the Eq. (12), using σ_{so}=173 mV, ρ_2=−0.189, ρ_3=0.0345 V, and $\bar{\Phi}_{bo}$=1.41 eV values.

200 K to 400 K as a function of forward bias according to the Eq. (12). The plots are given in Fig. 9. This plot says that Φ_{ap} increases with an increase in temperature at a given bias voltage. Then, it has been drawn Fig. 10. This figure shows the theoretical current versus temperature plots from 200 to 400 K as a function of forward bias according to the Eqs. (4), (5), and (12). For the sake of simplicity, it has been assumed R=0 while doing the calculations. This plot points out that the forward current increases with increase in temperature at a given bias voltage. Moreover, Fig. 11 shows the theoretical forward bias current-voltage plots according to the Eqs. (4), (5), and (12) in temperature ranges of 260–400 K. The calculations above have been made using σ_{so}=173 mV, ρ_2=0.189, ρ_3=−0.0345 V, and $\bar{\Phi}_{bo}$=1.41 eV values obtained from the experimental $[(1/n_{ap})\text{-}1]$ versus $1/T$ and Φ_{ap} versus $1/T$ curves belonging to the Ni/n-GaN SBD in Fig. 7. The obtained plots clearly show the solution of the ambiguity stated above.

In conclusion, a detailed analysis of the temperature dependence of the I-V and C-V characteristics of the Ni/n-GaN

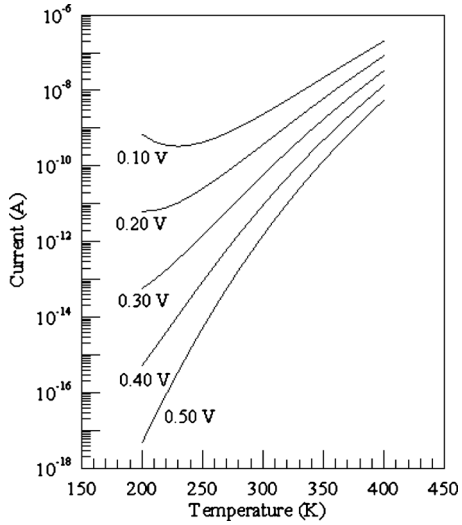

FIG. 10. Theoretical current vs temperature plots from 200 to 400 K as a function of forward bias according to the Eqs. (4), (5), and (12), using σ_{so}=173 mV, ρ_2=−0.189, ρ_3=0.0345 V, and $\bar{\Phi}_{bo}$=1.41 eV values.

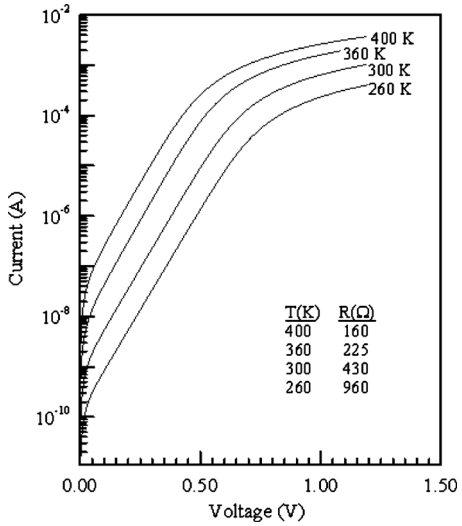

FIG. 11. Theoretical forward bias current-voltage plots according to the Eqs. (4), (5), and (12) in temperature ranges of 260–400 K, using σ_{so} =173 mV, ρ_2=−0.189, ρ_3=0.0345 V, and $\bar{\Phi}_{bo}$=1.41 eV values.

Schottky contacts prepared by magnetron DC sputtering has been made to determine the origin of the anomalous behavior of the BH and of the ideality factor and the Richardson's constant. The modified $\ln(I_0/T^2)$-$q^2\sigma_{so}^2/2k^2T^2$ versus $1/T$ plots obtained by a double-Gaussian distribution of BHs have yielded zero bias mean BH $\bar{\Phi}_{bo}$ of 0.72 eV (in the range of 100–200 K) and 0.142 eV (in the range of 200–400 K). These values are in agreement with exactly the mean BHs obtained from the Φ_{ap} versus $1/T$ plot. The modified activation energy plot from the barrier inhomogeneity model has given the values of 80 and 85 $A/(cm^2\ K^2)$ for the Richardson constant A^*. It has been seen that the obtained Richardson constant values are larger than the known value of 26.8 $A/(cm^2\ K^2)$ for n-type GaN.

ACKNOWLEDGMENTS

This work was supported by the Turkish Scientific and Technological Research Council of Turkey (TUBITAK) (Project No. 105T487) and Ataturk University (Project No. BAP 2006/51). The authors wish to thank to TUBITAK and Ataturk University.

[1]K. Suzue, S. N. Mohammad, Z. F. Fan, W. Kim, O. Aktas, A. E. Botchkarev, and H. Morkoc, J. Appl. Phys. **80**, 4467 (1996).
[2]J. Osvald, J. Kuzmik, G. Konstantinidis, P. Lobotka, and A. Georgakilas, Microelectron. Eng. **81**, 181 (2005).
[3]S. N. Mohammad, J. Appl. Phys. **97**, 063703 (2005).
[4]F. Lin, B. Shen, S. Huang, F. J. Xu, L. Lu, J. Song, F. H. Mei, N. Ma, Z. X. Qin, and G. Y. Zhang, J. Appl. Phys. **105**, 093702 (2009)
[5]A. Motayed and S. N. Mohammad, J. Chem. Phys. **123**, 194703 (2005).
[6]F. Iucolano, F. Roccaforte, F. Giannazzo, and V. Raineri, Appl. Phys. Lett. **90**, 092119 (2007); J. Appl. Phys. **102**, 113701 (2007).
[7]M. Mamor, J. Phys.: Condens. Matter **21**, 335802 (2009).
[8]K. Çınar, N. Yıldırım, C. Coşkun, and A. Turut, J. Appl. Phys. **106**, 073717 (2009).
[9]P. C. Chang, K. H. Lee, S. J. Chang, Y. K. Su, and C. H. Liu, Semicond. Sci. Technol. **24**, 105005 (2009).
[10]S. Huang, B. Shen, M. J. Wang, F. J. Xu, Y. Wang, H. Y. Yang, F. Lin, L. Lu, Z. P. Chen, Z. X. Qin, Z. J. Yang, and G. Y. Zhang, Appl. Phys. Lett. **91**, 072109 (2007).
[11]M. Ravinandan, P. K. Rao, and V. R. Reddy, Semicond. Sci. Technol. **24**, 035004 (2009); M. B. Reddy, V. Janardhanam, A. A. Kumar, V. R. Reddy, and P. N. Reddy, Curr. Appl. Phys. **10**, 687 (2010); M. S. P. Reddy, V. R. Reddy, and C. J. Choi, J. Alloys Compd. **503**, 186 (2010).
[12]L. Dobos, B. Pecz, L. Toth, Zs. J. Horvath, Z. E. Horvath, B. Beaumont, and Z. Bougrioua, Vacuum **82**, 794 (2008).
[13]C. J. Cheng, X. F. Zhang, Z. X. Lu, J. X. Ding, L. Zhang, L. Zhao, J. J. Si, W. G. Sun, L. W. Sang, Z. X. Qin, and G. Y. Zhang, Appl. Phys. Lett. **92**, 103505 (2008).
[14]T. Sawada, N. Kimura, K. Imai, K. Suzuki, and K. Tanahashi, J. Vac. Sci. Technol. B **22**, 2051 (2004); T. Sawada, Y. Ito, K. Imai, K. Suzuki, H. Tomozawa, and S. Sakai, Appl. Surf. Sci. **159–160**, 449 (2000).
[15]M. Diale and F. D. Auret, Physica B **404**, 4415 (2009); W. Mtangi, P. J. Janse van Rensburg, M. Diale, F. D. Auret, C. Nyamhere, J. M. Nel, and A. Chawanda, Mater. Sci. Eng., B **171**, 1 (2010).
[16]L. S. Yu, Q. Z. Liu, Q. J. Xing, D. J. Qiona, S. S. Lau, and J. Redwing, J. Appl. Phys. **84**, 2099 (1998).
[17]J. D. Guo, F. M. Pan, M. S. Feng, R. J. Guo, P. F. Chou, and C. Y. Chang, J. Appl. Phys. **80**, 1623 (1996).
[18]F. Iucolano, F. Roccaforte, F. Giannazzo, and V. Raineri, J. Appl. Phys. **104**, 093706 (2008).
[19]E. Arslan, S. Bütün, and E. Ozbay, Appl. Phys. Lett. **94**, 142106 (2009); E. Arslan, S. Altındal, S. Ozcelik, and E. Ozbay, Semicond. Sci. Technol. **24**, 075003 (2009).
[20]E. H. Rhoderick and R. H. Williams, *Metal-Semiconductor Contacts*, 2nd ed. (Clarendon M. A., Oxford, 1988).
[21]S. M. Sze, *Physics of Semiconductor Devices*, 2nd ed. (Wiley, New York, 1981), p. 850.
[22]J. P. Sullivan, R. T. Tung, M. R. Pinto, and W. R. Graham, J. Appl. Phys. **70**, 7403 (1991).
[23]J. H. Werner and H. H. Güttler, J. Appl. Phys. **69**, 1522 (1991).
[24]Y. P. Song, R. L. Van Meirhaeghe, W. H. Laflére, and F. Cardon, Solid-State Electron. **29**, 633 (1986).
[25]S. Arulkumaran, T. Egawa, H. Ishikawa, M. Umeno, and T. Jimbo, IEEE Trans. Electron Devices **48**, 573 (2001).
[26]Y. Zhou, D. Wang, C. Ahyi, C.-C. Tin, J. Williams, M. Park, N. M. Williams, A. Hanser, and E. A. Preble, J. Appl. Phys. **101**, 024506 (2007).
[27]A. R. Arehart, B. Moran, J. S. Speck, U. K. Mishra, S. P. DenBaars, and S. A. Ringel, J. Appl. Phys. **100**, 023709 (2006).
[28]S. Chand and J. Kumar, J. Appl. Phys. **82**, 5005 (1997); S. Chand and S. Bala, Appl. Surf. Sci. **252**, 358 (2005); S. Chand and J. Kumar, Appl. Phys. A: Mater. Sci. Process. **65**, 497 (1997).
[29]A. Gümüş, A. Turut, and N. Yalcın, J. Appl. Phys. **91**, 245 (2002).
[30]Z. Tekeli, Ş. Altındal, M. Çakmak, S. Özçelik, D. Çalışkan, and E. Özbay, J. Appl. Phys. **102**, 054510 (2007).
[31]S. Zhu, R. L. Van Meirhaeghe, C. Detavernier, F. Cordon, G. P. Ru, X. P. Qu, and B. Z. Li, Solid-State Electron. **44**, 663 (2000).
[32]J. Osvald, J. Appl. Phys. **85**, 1935 (1999); E. Dobrocka and J. Osvald, Appl. Phys. Lett. **65**, 575 (1994); J. Osvald, Solid-State Electron. **50**, 228 (2006).
[33]B. Abay, G. Cankaya, H. S. Guder, H. Efeoglu, and Y. K. Yogurtcu, Semicond. Sci. Technol. **18**, 75 (2003).
[34]M. E. Aydin, K. Akkiliç, and T. Kiliçoglu, Appl. Surf. Sci. **225**, 318 (2004).
[35]Zs. J. Horvath, V. Rakovics, B. Szentpali, S. Püpoki, and K. Zdansky, Vacuum **71**, 113 (2003); E. Ayyildiz, H. Cetin, and Zs. J. Horvath, Appl. Surf. Sci. **252**, 1153 (2005).
[36]N. Yıldırım and A. Turut, Microelectron. Eng. **86**, 2270 (2009).
[37]F. Yakuphanoglu and B. F. Senkal, Synth. Met. **158**, 821 (2008).
[38]N. Yıldırım, A. Turut, and V. Turut, Microelectron. Eng. **87**, 2225 (2010).
[39]C. Lu and S. N. Mohammad, Appl. Phys. Lett. **89**, 162111 (2006).
[40]T. P. Chen, T. C. Lee, C. C. Ling, C. D. Beling, and S. Fung, Solid-State Electron. **36**, 949 (1993).
[41]M. O. Aboelfotoh, J. Appl. Phys. **66**, 262 (1989).
[42]M. Soylu and B. Abay, Microelectron. Eng. **86**, 88 (2009).
[43]S. Zhu, R. L. Van Meirhaeghe, C. Detavernier, G. P. Ru, B. Z. Li, and F. Cordon, Solid State Commun. **112**, 611 (1999).
[44]M. Campos and P. A. P. Nascente, Synth. Met. **160**, 1513 (2010).